Journal Article

Design and Performance Study of a Dual-Element Multiband Printed Monopole Antenna Array for MIMO Terminals

Shoaib, S., Shoaib, I., Shoaib, N., Chen, X. and Parini, C. G.

Design and Performance Study of a Dual-Element Multiband Printed Monopole Antenna Array for MIMO Terminals

Sultan Shoaib, Imran Shoaib, *Student Member, IEEE*, Xiaodong Chen, *Senior Member, IEEE*, Nosherwan Shoaib, and Clive G. Parini, *Member, IEEE*

***Abstract*—This paper presents a study on linearly polarized compact multiband multiple–input multiple–output (MIMO) antenna system for small mobile terminals. The MIMO antenna system consists of two symmetric printed monopole antennas with edge-to-edge separation of $0.097\lambda_0$ at 900 MHz. Each antenna element has a capacitive feed and is composed of two twisted lines, a parasitic loop, and a shorting trip that generate five resonant modes around 900, 1800, 2100, 3500, and 5400 MHz, covering GSM850/900, DCS, PCS, UMTS, WLAN and WiMAX frequency bands. Two inverted-L shaped branches and a rectangular slot with one circular end, etched on the ground plane, were introduced to improve the isolation between antenna elements. The isolation achieved is higher than 15 dB in the lower band and 20 dB in the upper bands, leading to an envelope correlation coefficient of less than 0.025. The simulated performance of the designed antenna system has been verified in the experiment.**

***Index Terms*—Antenna, decoupling, envelope correlation co-efficient, multiband antenna, multiple-input multiple-output (MIMO) antenna, printed monopole antenna.**

I. Introduction

THE multiple-input multiple-output (MIMO) is a key technology for modern wireless communication standards, such as Long Term Evolution (LTE), wireless LAN (IEEE 802.11n), and Worldwide Interoperability for Microwave Access (WiMAX). Studies [1], [2] have demonstrated that the MIMO technology can substantially improve the network throughput, capacity and coverage without requiring additional bandwidth. At the same time, portable wireless terminals have been developed to have numerous functions, supporting multiple standards on a smaller handset. It is, therefore, necessary to develop compact multi-band antennas to support multi-functional MIMO-enabled wireless terminals.

Manuscript received Month 01, 2013; revised Month 01, 2013; accepted Month 01, 2013. Date of publication Month 01, 2013; date of current version Month 01, 2013.

S. Shoaib, I. Shoaib, X. Chen and C. G. Parini are with the School of Electronic Engineering and Computer Science, Queen Mary University of London, United Kingdom (e-mail: ss311@eecs.qmul.ac.uk).

N. Shoaib is with the Department of Electronics and Telecommunications, Politecnico Di Torino, Turin, Italy (e-mail: nosherwan.shoaib@polito.it).

Color versions of one or more of the figures in this letter are available online at http://ieeexplore.ieee.org.

Digital Object Identifier

Recently, several antenna designs have been proposed in the literature for use in MIMO terminals. A dual-element printed monopole antenna developed for 2.5–2.7 GHz band, using neutralization line for decoupling, was reported in [3]. In [4], a dual-band printed diversity antenna for mobile terminals with UMTS and 2.4 GHz WLAN operations was studied. The antenna consists of two back-to-back monopoles printed on a printed circuit board with several ground branches to increase isolation and adjust the resonant frequency. A dual-element folded monopole antenna for 2.4/5.6 GHz operation was proposed in [5]. In this case, isolation was achieved by printing two transmission lines on the top surface of the substrate and etching two slots on the ground. Multiband antennas were also developed for mobile terminals, such as [6] designed to operate in the 2.4/3.5/5.25/5.8 GHz bands and [7] that can operate in the 2.4/5.2/5.8 GHz WLAN, 2.5/3.5/5.5 GHz WiMAX and the lower 3.1–4.8 GHz UWB band. In [7], two bent slits were etched on the ground plane to reduce coupling and improve impedance matching. More recently, low-frequency MIMO antenna systems for GSM850/900/ DCS/PCS/UMTS/LTE2500 and GSM 900/1800/1900/UMTS were proposed in [8] and [9], respectively. In all cases the antennas support a selective range of frequencies.

In this paper, we present a compact linearly polarized dual-element printed MIMO antenna system that was developed to support the GSM850/900, DCS, PCS, UMTS, WLAN, and WiMAX frequencies. The proposed antenna solution was realized using an array of two printed monopoles [10], illustrated in Fig. 1. A novel decoupling structure, consisting of two inverted-L branches and a rectangular slot with one circular end, etched on the ground plane, was introduced to achieve low mutual coupling below -15 dB for all matched frequency bands. The following section presents the details of MIMO antenna configuration followed by a discussion on the results, including the effect of the decoupling structure on the isolation between antenna elements.

II. MIMO Antenna Configuration

The geometry of the proposed multiband MIMO antenna configuration, with decoupling network, is shown in Fig. 1. The multiband MIMO antenna, consisting of two printed monopole antenna elements [10] with symmetric configuration and edge-to-edge separation of 32.4 mm (i.e.

$0.097\lambda_0$ at 900 MHz), was printed on the top layer of a $125\times85\times0.8$ mm^3 FR4 substrate with relative permittivity of 4.4 and loss tangent of 0.02. The detailed dimensions of the individual printed monopole antenna elements are illustrated in Fig. 1(c). Each printed monopole antenna element consists of a capacitive feed (AB section) connected to a 50Ω microstrip feed line at point A, two twisted lines (DF and EG section), a parasitic loop (MN section), and a shorting strip (IH section). Each printed monopole antenna element can generate five resonant modes around 900, 1800, 2100, 3500, and 5400 MHz. The first three resonant modes can be

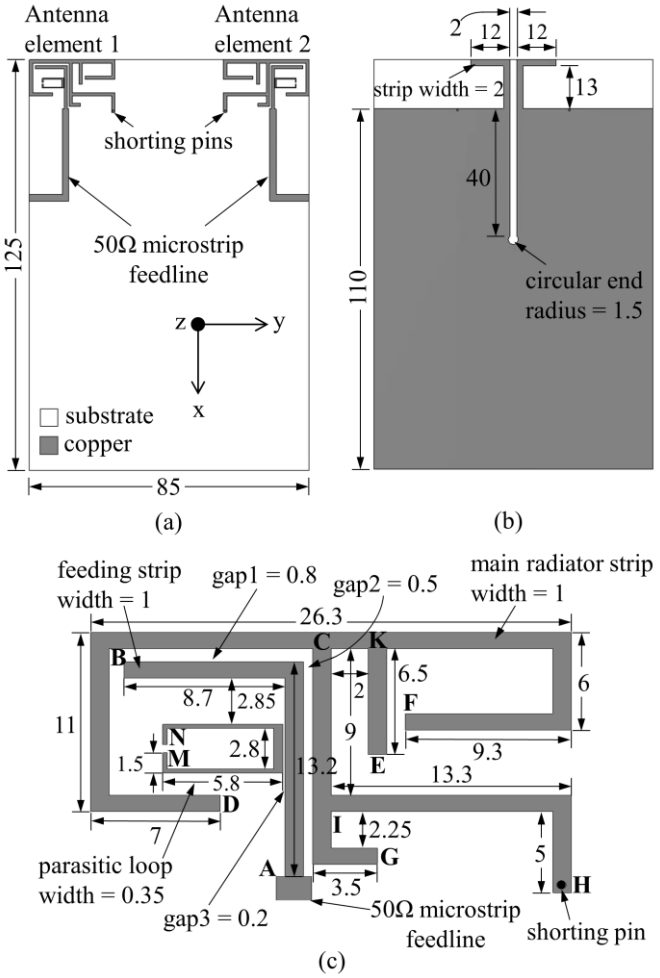

Fig. 1. The proposed MIMO antenna configuration with decoupling network: (a) Top layer, (b) Bottom layer, and (c) Dimensions of the individual monopole antenna elements (Units: millimeters).

generated by using the DF twisted line combined with the shorting strip and the CI section. The EG section passing through points K, C, and I generate the fourth resonant mode around 3500 MHz to cover the 3400 to 3600 MHz WiMAX frequency band. The fifth and last resonant mode at 5400 MHz is generated through the parasitic loop MN, which allows the antenna to support WLAN in Europe.

The decoupling structure, consisting of two inverted-L branches and a rectangular slot with one circular end, was etched on the ground plane which is the bottom layer of the substrate. Low mutual coupling below -15 dB was achieved for all matched frequency bands. The mechanism for decoupling is that the two inverted-L branches combined with the etched slot block the current flowing from the excited port to the coupled port. The proposed MIMO antenna system was optimized using CST Microwave Studio® [11].

III. Simulation and Experimental Results

To validate the simulation, a prototype of the proposed multiband MIMO antenna was fabricated according to the optimized dimensions and measured using Agilent N5230C PNA-L microwave network analyzer. Shown in Fig. 2 is the photograph of the fabricated antenna prototype.

The measured and simulated $|S_{11}|$ and $|S_{21}|$ of the proposed

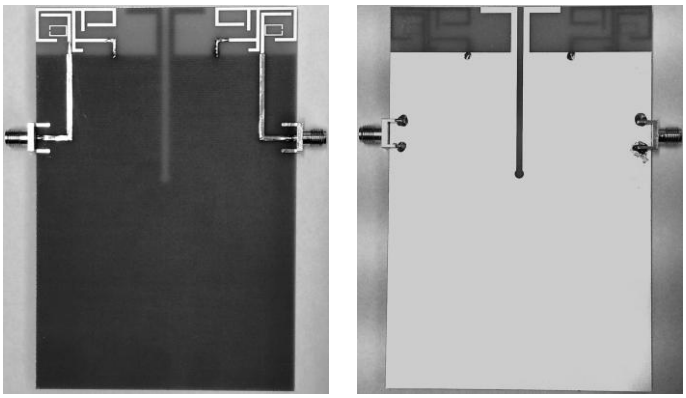

(a) (b)

Fig. 2. Photograph of the multiband MIMO antenna prototype: (a) Top layer, and (b) Bottom layer.

MIMO antenna configuration are shown in Fig. 3 and Fig. 4, respectively. The $|S_{22}|$ and $|S_{12}|$ are not shown because the two antenna elements are symmetrical. The bandwidth of the proposed antenna determined by VSWR 3:1 and the respective wireless applications are listed in Table I. It is observed that the antenna is well matched over the desired frequency bands and the difference between the measured and simulated results is probably due to the fabrication imperfections and the tolerance due to the permittivity of the substrate. The measured $|S_{21}|$ is lower than -15 dB in the first Band (826–1005 MHz) and below -20 dB over the other Bands (1527–5749 MHz) covered by the antennas.

TABLE I
List of Frequencies supported by the Proposed MIMO Antenna

Frequency (MHz)	Wireless Applications
826–1005	GSM850 (824–894 MHz) GSM900 (880–960 MHz)
1527–2480	DCS (1710–1880 MHz), PCS (1850–1990 MHz) UMTS (1920–2170 MHz), WLAN (2400–2480 MHz)
3439–3690	WiMAX (3400–3600 MHz)
5340–5749	WLAN (5470–5725 MHz)

The measured and simulated theta and phi normalized radiation patterns of antenna element 1 in x-z and y-z planes at 0.9, 2.1, 3.5 and 5.4 GHz are shown in Fig. 5, while the antenna element 2 is terminated with a 50Ω matched load.

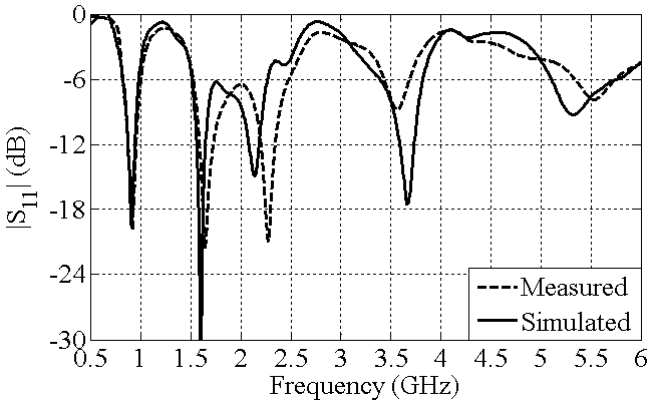

Fig. 3. Measured and simulated $|S_{11}|$ of the proposed MIMO antenna configuration.

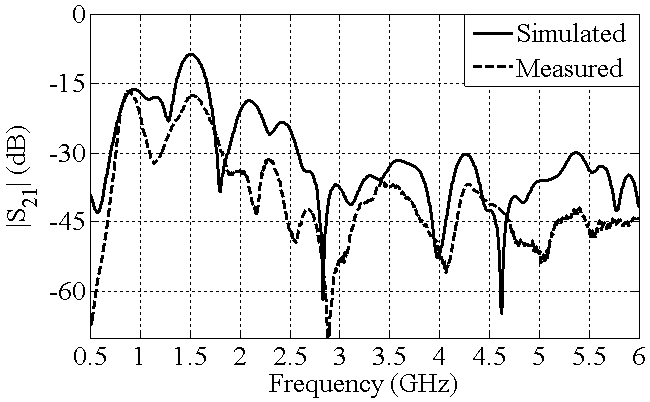

Fig. 4. Measured and simulated $|S_{21}|$ of the proposed MIMO antenna configuration.

The radiation patterns of antenna element 2 are not shown as the two antenna elements are symmetric. The discrepancy between the measured and simulated results is primarily caused by our measurement setup which also includes the connecting cables and also the imperfections in fabrication.

The envelope correlation coefficient is an important parameter for a MIMO antenna system, which can be calculated using far-field radiation patterns [12] and through S-parameters under the assumptions that the incoming signals are uniformly distributed and the antenna elements are lossless and well matched [13]. The peak envelope correlation coefficient for the proposed MIMO antenna system in four different bands is calculated and listed in Table II. The Envelope correlation coefficient is calculated using both radiation pattern and the S-parameters in order to check the accuracy of the S-parameters method. The maximum value of the envelope correlation coefficient over all matched frequency bands is observed to be 0.025, which is well below the acceptable value of 0.5.

The simulated radiation efficiency of the antenna element 1 is 86.2%, 97.9%, 82.9 and 72.2% in the first, second, third and fourth band respectively. The simulated radiation efficiency of the antenna is lower at the fourth band (5340-5749 MHz) and higher on the other bands. This is because the return loss is good at lower bands as compared to the upper band. As return loss gets worse the radiation efficiency gets lower. The simulated radiation efficiencies are also mentioned in table II.

TABLE II
PEAK ENVELOPE CORRELATION COEFFICIENT AND RADIATION EFFICIENCY

Bandwidth	Envelope Correlation Coefficient			Radiation Efficiency (%)
	Using Radiation Pattern	Using S-parameter		
	Simulated	Simulated	Measured	
826–1005	0.0186	0.0206	0.0184	86.2
1527–2480	0.0253	0.0092	0.0008	97.9
3439–3690	0.0005	0.0003	0.0003	82.9
5340–5749	0.0012	0.0006	0.0001	72.2

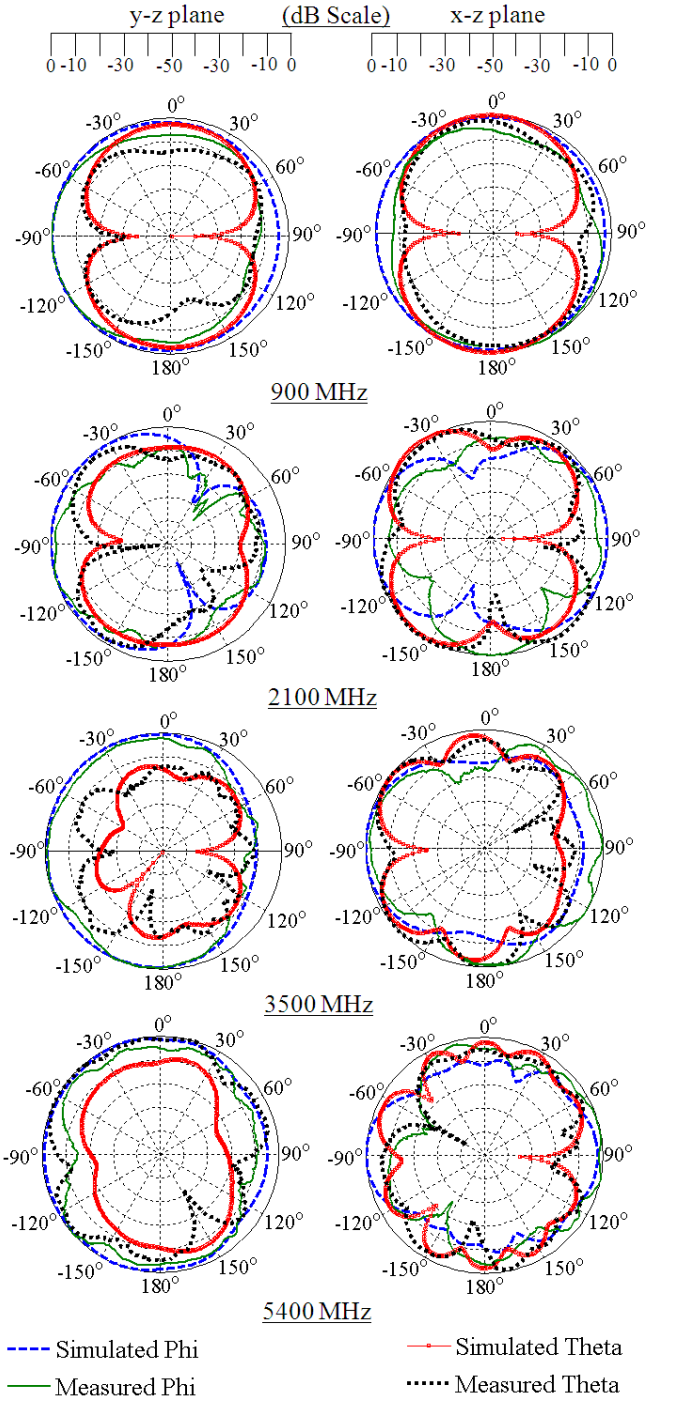

Fig. 5. Measured and simulated normalized radiation patterns of the antenna element 1 at: (a) 0.9 GHz, (b) 2.1 GHz, (c) 3.5 GHz, and (d) 5.4 GHz.

IV. Study of Decoupling Structure

In this paper, a decoupling structure consisting of two inverted-L branches and a rectangular slot with one circular end, etched on the ground plane, was introduced to reduce the mutual coupling between the two antenna elements. The proposed mechanism for decoupling using two inverted-L branches combined with the etched slot block the current flowing from the excited port to the coupled port. To explain

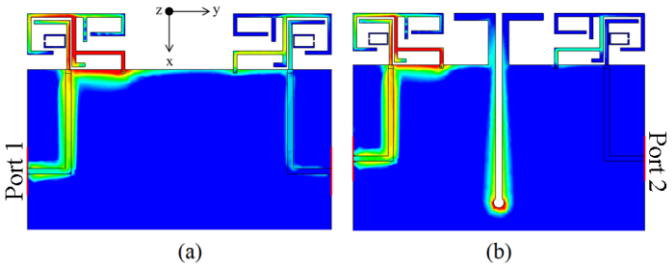

Fig. 6. Simulated surface current distribution on the MIMO antenna system at 900 MHz (a) without and (b) with decoupling structure.

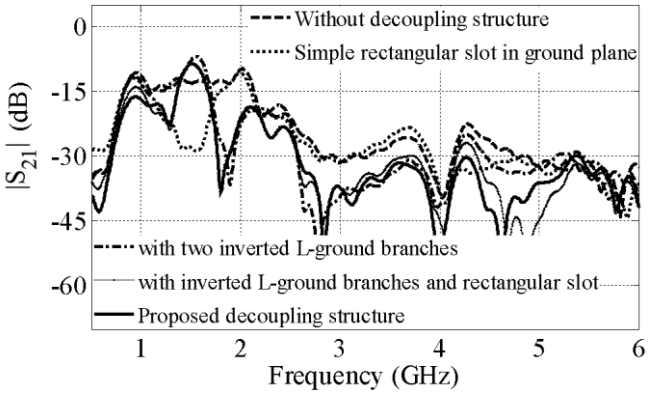

Fig. 7. Simulated $|S_{21}|$ of the proposed MIMO antenna configuration with different elements of the decoupling structure.

this further, the simulated surface current distribution on the MIMO antenna both with and without the decoupling structure at 900 MHz is shown in Fig. 6. It can be seen that the current flowing into port 2 is significantly reduced by introducing the decoupling structure as compared to the current flowing into port 2 when there is no decoupling structure between the two antenna elements of the MIMO configuration. The depth of rectangular slot, radius of circular end and the length of inverted-L branches were optimized for the lowest coupling. Fig. 7 shows the change in coupling between the two antenna elements with the introduction of individual elements of the proposed decoupling structure. It can be observed that without the decoupling structure the $|S_{21}|$ is higher than -15 dB in the first (826–1005 MHz) and second (1527–2480 MHz) frequency bands, which is considered as poor isolation in the case of a mobile terminal. The isolation in second band improved significantly when the two inverted-L branches were introduced, while there is a slight improvement of isolation in the first band. The isolation in first band covered by the antennas increased to above 15 dB when the two inverted-L branches and the rectangular slot with circular end were combined to form a single decoupling structure. The effect of the proposed decoupling structure on input reflection coefficient of individual antenna elements was negligible.

V. Conclusions

A compact and multiband MIMO antenna system covering GSM 850/900, DCS, PCS, UMTS, WLAN, and WiMAX bands has been studied in this letter. The MIMO antenna system is consisted of two symmetric printed monopole antennas and a decoupling network. Both simulation and measurements have corroborated a good performance of the MIMO antenna system. The isolation achieved is greater than 15 dB in the lower band and 20 dB in the upper bands, leading to an envelope correlation coefficient of less than 0.025. This simple and low cost design is promising for mobile terminals. However, more work can be done to reduce the width of the PCB by changing the orientation of the antenna elements and the decoupling structure.

References

[1] G. J. Foschini and M. J. Gans, "On limits of wireless communications in a fading environment when using multiple antennas," *Wireless Personal Commun.*, vol. 6, no. 3, pp. 311–335, Mar. 1998.

[2] T. Bolin, A. Derneryd, G. Kristensson, V. Plicanic, and Z. Ying, "Two-antenna receive diversity performance in indoor environment," *IEEE Electron. Lett.*, vol. 41, no. 2, pp. 1205–1206, Oct. 2005.

[3] V. Ssorin, A. Artemenko, A. Sevastyanov, and R. Maslennikov, "Compact bandwidth-optimized two element MIMO antenna system for 2.5–2.7 GHz band," in *Proc. Eur. Conf. Antennas Propag.*, 2011, pp. 319–323.

[4] Y. Ding, Z. Du, K. Gong, and Z. Feng, "A novel dual-band printed diversity antenna for mobile terminals," *IEEE Trans. Antennas Propag.*, vol. 55, no. 7, pp. 2088–2096, Jul. 2007.

[5] S. Cui, Y. Liu, W. Jiang, and S.X. Gong, "Compact dual-band monopole antennas with high port isolation," *Electron. Lett.*, vol. 47, no. 10, pp. 579–580, May 2011.

[6] R. A. Bhatti, J.-H. Choi, and S.-O. Park, "Quad-band MIMO antenna array for portable wireless communications terminals," *IEEE Antennas Wireless Propag. Lett.*, vol. 8, pp. 129–132, 2009.

[7] J.-F. Li, Q.-X. Chu, and T.-G. Huang, "A compact wideband MIMO antenna with two novel bent slits," *IEEE Trans. Antennas Propag.*, vol. 60, no. 12, pp. 482–489, Feb. 2012.

[8] C. Yang, Y. Yao, J. Yu, and X. Chen, "Novel compact multiband MIMO antenna for mobile terminal," *Int. J. Antennas Propag.*, vol. 2012, article ID 691681, pp. 1–9, 2012.

[9] Q. Zeng, Y. Yao, S. Liu, J. Yu, P. Xie, and X. Chen, "Tetraband small-size printed strip MIMO antenna for mobile handset application," *Int. J. Antennas Propag.*, vol. 2012, article ID 320582, pp. 1–8, 2012.

[10] J. Ma, Y. Z. Yin, J. L. Guo, and Y. H. Huang, "Miniature printed octaband monopole antenna for mobile phones," *IEEE Antennas Wireless Propag. Lett.*, vol. 9, pp. 1033–1036, 2010.

[11] CST Microwave Studio®, Computer Simulation Technology Homepage [Online]. Available: http://www.cst.com

[12] R. G. Vaughan and J. B. Anderson, "Antenna diversity in mobile communications," *IEEE Trans. Veh. Technol.*, vol. 36, no. 4, pp. 149–172, 1987.

[13] S. Blanch, J. Romeu, and I. Corbella, "Exact representation of antenna system diversity performance from input parameter description," *Electron. Lett.*, vol. 39, no. 9, pp. 705–707, May 2003.